J Therm Anal Calorim (2011) 105:867–871
DOI 10.1007/s10973-011-1370-7

Synthesis, characterization and thermal behaviour of solid-state tartrates of heavy trivalent lanthanides and yttrium(III)

B. Ambrozini · P. R. Dametto · M. Ionashiro

ESTAC2010 Conference Special Issue

Abstract Solid state Ln_2-L_3 compounds, where Ln stands for heavy trivalent lanthanides (terbium to lutetium) and yttrium, and L is tartrate $[(C_4H_4O_6)^{-2}]$ have been synthesized. Simultaneous thermogravimetry and differential thermal analysis, differential scanning calorimetry, X-ray powder diffractometry, infrared spectroscopy, elemental analysis and complexometry were used to characterize and to study the thermal behaviour of these compounds. The results provided information concerning the stoichiometry, crystallinity, ligand's denticity, thermal stability and thermal behaviour of these compounds.

Keywords Heavy lanthanides · Tartrate · Characterization · Thermal behaviour

Introduction

Tartaric acid (dihydroxybutanedioic acid) is an organic compound which has not an ample utilization as citric and malic acids, but it has a great importance in the provision industry. It is used as acidulant in some food [1].

Tartaric acid ($C_4H_6O_6$) is found in grapes in the form L (+). Amongst all the organic acids present in grapes it is found in greater quantities than the others [2].

A survey of literature shows that the thermal studies involving compounds derivate of tartrate, the studies reported the thermal decomposition and kinetics of dehydration of praseodimium (III), neodymium (III) and gadolinium (III) tartarates [3, 4], TG and DSC studies on Sm(III) and Tb(III) tartrates [5], thermal decomposition behaviour of lanthanium (III) tris–tartrato lanthanate (III) decahydrate [6], studies on kinetics and mechanism of thermal decomposition of yttrium tartrate trihydrate crystals [7] and kinetics and mechanism of thermal decomposition of strontium tartrate crystals [8] and thermal behaviour of solid-state tartrate of some trivalent metal ions have also been described [9].

In this article, solid-state compounds of heavy trivalent lanthanides (Tb to Y) with tartrate $[(C_4H_4O_6)^{-2}]$ were synthesized. The compounds were investigated by complexometry, elemental analysis, X-ray powder diffractometry, infrared spectroscopy, simultaneous thermogravimetry and differential thermal analysis (TG-DTA) and differential scanning calorimetry (DSC). The results allowed us to acquire information concerning these compounds in the solid state including their thermal stability and crystallinity. This article is a continuation of the study of reference [9].

Experimental

The sodium tartrate with 99% purity was obtained from Sigma-Aldrich. Aqueous solution of sodium tartrate 0.20 mol L^{-1} was made by direct weighing of the solid salt. Aqueous solutions of bivalent metal ions 0.20 mol L^{-1} were prepared by dissolving the corresponding chlorides.

Heavy lanthanide chlorides were prepared from the corresponding metal oxides by treatment with concentrated hydrochloric acid. The resulting solutions were evaporated to near dryness; the residues were again dissolved in distilled water, transferred to a volumetric flask and diluted into obtain ca. 0.1 mol L^{-1} solutions, whose pH were adjusted to 5.0 by adding diluted sodium hydroxide or hydrochloric acid solutions.

B. Ambrozini · P. R. Dametto (✉) · M. Ionashiro
Instituto de Química, UNESP, C. P. 355, Araraquara, SP CEP 14801-970, Brazil
e-mail: pdametto@gmail.com

Table 1 Analytical data for the $Ln_2(L)_3{\cdot}nH_2O$

Compounds	Water/%		Ligand lost/%		Metal oxide/%			Carbon/%		Hydrogen/%		Residue
	Calcd.	TG	Calcd.	TG	Calcd.	TG	EDTA	Calcd.	E.A.	Calcd.	E.A.	
$Tb_2(L)_3{\cdot}4H_2O$	8.07	8.06	54.90	54.47	45.10	45.72	45.53	17.39	17.23	2.44	2.42	Tb_4O_7
$Dy_2(L)_3{\cdot}4H_2O$	7.65	7.64	55.21	54.31	45.34	45.52	45.65	17.30	17.00	2.42	2.39	Dy_2O_3
$Ho_2(L)_3{\cdot}3H_2O$	6.93	6.53	54.57	53.76	45.43	45.80	46.23	17.33	17.04	2.18	2.15	Ho_2O_3
$Er_2(L)_3{\cdot}4H_2O$	7.68	7.49	54.65	53.82	45.14	45.62	45.68	17.08	16.84	2.37	2.33	Er_2O_3
$Tm_2(L)_3{\cdot}5H_2O$	9.55	9.34	55.37	54.98	44.62	45.02	45.48	16.66	16.59	2.57	2.55	Tm_2O_3
$Yb_2(L)_3{\cdot}4H_2O$	8.72	8.74	54.48	54.80	44.78	45.14	45.22	16.64	16.75	2.33	2.34	Yb_2O_3
$Lu_2(L)_3{\cdot}5H_2O$	10.13	10.20	54.97	54.69	45.03	45.29	44.35	16.31	16.18	2.51	2.50	Lu_2O_3
$Y_2(L)_3{\cdot}5H_2O$	12.73	12.12	68.10	67.66	31.90	32.32	32.64	20.36	20.42	3.14	3.12	Y_2O_3

Ln heavy lanthanides (III) and yttrium (III), *L* tartrate ($C_4H_4O_6^{-2}$)

The solid-state compounds were prepared by adding slowly, with continuous stirring, the solution of the ligand to the respective metal chloride until total precipitation of the metal ions. The precipitates were washed with distilled water until elimination of chloride ions (qualitative test with $AgNO_3/HNO_3$ solution), filtered through and dried on Whatman no 42 filter paper and kept in a desiccator over anhydrous calcium chloride.

In the solid-state compounds hydration water, ligand and metal ion content were determined from TG curves. The metal ions were also determined by complexometric titrations with standard EDTA solution using xylenol orange as indicator after igniting the compounds to the respective oxides and their dissolution in hydrochloric acid [10].

X-ray powder patterns were obtained by using a SIEMENS D-5000 X-ray diffractometer employing CuK_α radiation ($\lambda = 1.541$ Å) and setting of 40 kV and 20 mA.

The attenuate total reflectance infrared spectra for sodium tartrate and for its metal-ion compounds were run on a Nicolet iS10 FT-IR spectrophotometer, using an ATR accessory with Ge window.

Simultaneous TG-DTA and DSC curves were obtained with two thermal analysis systems, models 2960 and Q10 both from TA Instruments, respectively. The purge gas was an air flow of 100 mL min^{-1} (TG-DTA) and 50 mL min^{-1} (DSC). A heating rate of 20 K min^{-1} and with samples weighing about 7 mg (TG-DTA) and about 5 mg (DSC). Alumina and aluminium crucibles, the latter with perforated cover were used for TG-DTA and DSC, respectively.

Carbon and hydrogen contents were determined by microanalytical procedures with an EA 1110 CHNS-O Elemental Analyser from CE Instruments.

Results and discussion

The analytical, thermoanalytical (TG) and elemental analysis results are shown in Table 1. These results establish the stoichiometry of these compounds, which are in agreement with the general formula $Ln_2(C_4H_4O_6)_3{\cdot}nH_2O$, where Ln represents trivalent heavy lanthanides (Tb to Lu) or Y and $n = 3.0$ (Ho), 4.0 (Tb, Dy, Er and Yb) or 5.0 (Tm, Lu and Y).

Table 2 Spectroscopic data for sodium tartrate and compounds with heavy trivalent lanthanides

Compounds	$\nu_{as(COO^-)}/cm^{-1}$	$\nu_{s(COO^-)}/cm^{-1}$	$\nu(\nu_{as}-\nu_s)/cm^{-1}$
Na(L)	1622_s	1409_s	213
$Tb_2(L)_3{\cdot}4H_2O$	1595_s	1388_s	207
$Dy_2(L)_3{\cdot}4H_2O$	1597_s	1391_s	206
$Ho_2(L)_3{\cdot}3H_2O$	1597_s	1391_s	206
$Er_2(L)_3{\cdot}4H_2O$	1622_s	1419_s	203
$Tm_2(L)_3{\cdot}5H_2O$	1600_s	1408_s	192
$Yb_2(L)_3{\cdot}4H_2O$	1602_s	1412_s	190
$Lu_2(L)_3{\cdot}5H_2O$	1602_s	1414_s	188
$Y_2(L)_3{\cdot}5H_2O$	1602_s	1410_s	192

s strong; *L* tartrate ($C_4H_4O_6^{-2}$)

$\nu_{s(COO-)}$ and $\nu_{as(COO-)}$ symmetrical and anti-symmetrical vibrations of the COO^- structure

X-ray powder patterns showed that all the compounds were obtained in amorphous state. The amorphous state is undoubtedly related to the low solubility of these compounds.

Infrared spectroscopic data on sodium tartrate ($Na_2C_4H_4O_6$) and its compounds with the metal ions considered in this study are shown in Table 2. The investigation was focused mainly within the 1700–1400 cm^{-1} range because the region is potentially most informative in attempting to assign coordination sites. In the $Na_2C_4H_4O_6$, strong bands located at 1622 and 1409 cm^{-1} are attributed to anti-symmetrical (ν_{as}) and symmetrical (ν_{sym}) frequencies of the carboxylate groups, respectively [11, 12]. For the synthesized compounds the band assigned to the anti-symmetrical stretching carboxylate frequencies are shifted to lower values and the symmetrical ones to higher, relative to the corresponding frequencies in $C_4H_6O_6$. The $\Delta\nu$ (ν_{as}–

ν_s) for these compounds is indicative that these lanthanides are linked to the carboxylate group by a bidentate bond with an incomplete equalization of bond lengths in the carboxylate anion [13].

Simultaneous TG-DTA curves of the compounds are shown in Fig. 1. These curves exhibit mass losses in four (Tb, Dy, Ho, Er, Tm, Yb, Lu and Y) steps between 303 and 1263 K. The first mass loss between 303 and 463 K (Tb–

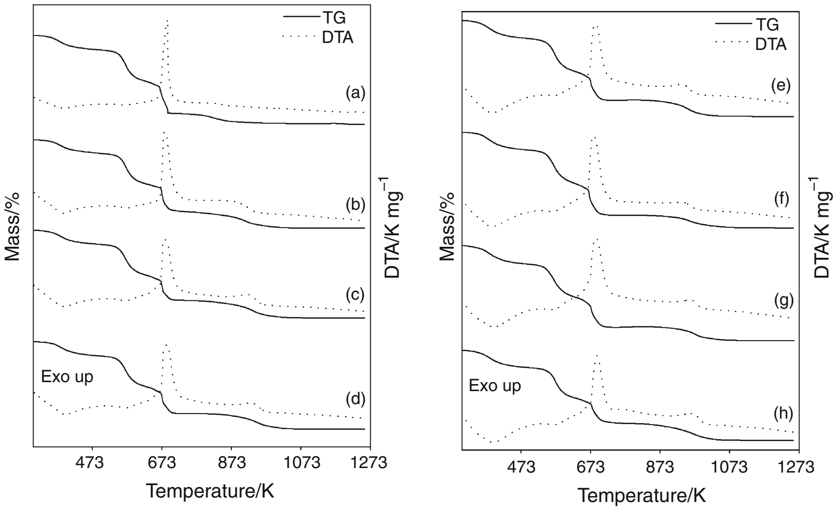

Fig. 1 TG-DTA curves of: *a* $Tb_2(L)_3{\cdot}4H_2O$; *b* $Dy_2(L)_3{\cdot}4H_2O$; *c* $Ho_2(L)_3{\cdot}3H_2O$; *d* $Er_2(L)_3{\cdot}4H_2O$; *e* $Tm_2(L)_3{\cdot}5H_2O$; *f* $Yb_2(L)_3{\cdot}4H_2O$; *g* $Lu_2(L)_3{\cdot}5H_2O$; *h* $Y_2(L)_3{\cdot}5H_2O$. *L* tartrate ($C_4H_4O_6^{-2}$)

Table 3 Temperature ranges (*T*), mass losses (%) and peak temperature observed for each step of the TG-DTA curves of the compounds $Ln_2(L)_3{\cdot}nH_2O$ where *Ln* trivalent lanthanides and yttrium, *L* tartrate

Compounds		Steps			
		First	Second	Third	Fourth
$Tb_2(L)_3{\cdot}4H_2O$	*T* (K)	303–453	453–663	663–688	688–1263
	Loss (%)	8.07	23.40	16.54	6.46
	Peak (K)	393	573	683	823
$Dy_2(L)_3{\cdot}4H_2O$	*T* (K)	303–453	453–668	668–698	698–1048
	Loss (%)	7.65	21.81	14.54	10.11
	Peak (K)	383	568	693	873
$Ho_2(L)_3{\cdot}3H_2O$	*T* (K)	303–423	423–673	673–698	698–1063
	Loss (%)	6.93	24.32	11.35	11.15
	Peak (K)	393	570	687	910
$Er_2(L)_3{\cdot}4H_2O$	*T* (K)	303–443	443–673	673–703	703–1063
	Loss (%)	7.68	24.07	12.04	10.03
	Peak (K)	396	573	691	933
$Tm_2(L)_3{\cdot}5H_2O$	*T* (K)	303–463	463–673	673–703	703–1053
	Loss (%)	9.55	27.61	9.80	8.02
	Peak (K)	390	572	686	938
$Yb_2(L)_3{\cdot}4H_2O$	*T* (K)	303–433	433–663	663–703	703–1063
	Loss (%)	8.72	21.39	14.26	10.43
	Peak (K)	390	568	683	943
$Lu_2(L)_3{\cdot}5H_2O$	*T* (K)	303–463	463–668	668–708	708–1088
	Loss (%)	10.13	20.47	12.04	12.05
	Peak (K)	393	566	688	964
$Y_2(L)_3{\cdot}5H_2O$	*T* (K)	303–463	463–673	673–708	708–1070
	Loss (%)	12.12	27.60	13.46	14.48
	Peak (K)	393	573	691	967

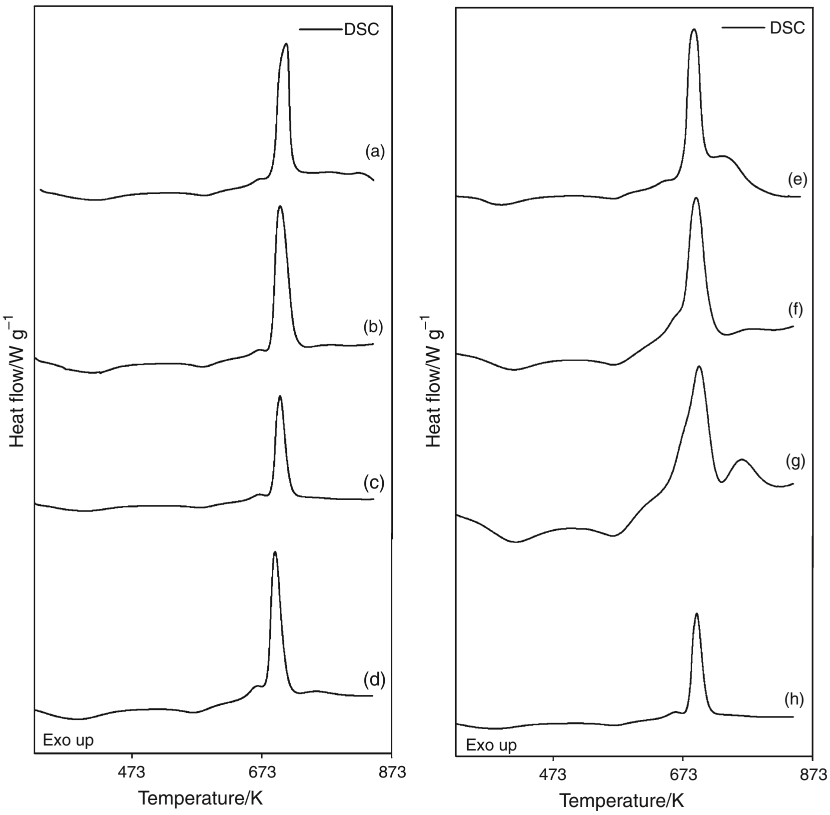

Fig. 2 DSC curves of:
a $Tb_2(L)_3 \cdot 4H_2O$;
b $Dy_2(L)_3 \cdot 4H_2O$;
c $Ho_2(L)_3 \cdot 3H_2O$;
d $Er_2(L)_3 \cdot 4H_2O$;
e $Tm_2(L)_3 \cdot 5H_2O$;
f $Yb_2(L)_3 \cdot 4H_2O$;
g $Lu_2(L)_3 \cdot 5H_2O$;
h $Y_2(L)_3 \cdot 5H_2O$. *L* tartrate
$(C_4H_4O_6^{-2})$

Y) corresponding to the endothermic peak at 393 K (Tb), 383 K (Dy), 393 K (Ho), 396 K (Er), 390 K (Tm), 390 K (Yb), 393 K (Lu) and 393 K (Y) is due to dehydration, which occurs in a single step.

After dehydration the mass losses observed above 453 K (Tb), 453 K (Dy), 423 K (Ho), 443 K (Er), 463 K (Tm), 433 K (Yb), 463 K (Lu) and 463 K (Y) are due to the thermal decomposition of the anhydrous compounds; these take place in consecutive and/or overlapping steps with partial losses which are characteristic for each compound.

For theses compounds the mass loss up to 1263 K (Tb), 1048 K (Dy), 1063 K (Ho), 1063 K (Er), 1053 K (Tm), 1063 K (Yb), 1088 K (Lu) and 1070 K (Y) corresponding to endothermic or exothermic peaks attributed to the thermal decomposition being the exothermic events due to the oxidation of the organic matter (Fig. 1). Calculations based on the total mass losses observed in the TG curves are in agreement with the formation of the respective oxides, Tb_4O_7, Ln_2O_3 (L = Dy, Ho, Er, Tm, Yb, Lu and Y). The mass losses, temperature ranges and the peak temperatures observed in each step of the TG-DTA curves are shown in Table 3.

The DSC curves of the compounds are shown in Fig. 2. These curves show endothermic and exothermic peaks that all are in agreement with the mass losses observed in the TG curves. The endothermic peak at 383–443 K is assigned to the dehydration, which occurs in single step. The dehydration enthalpies found for the compounds (Tb–Y) were: 145.8, 157.9, 102.9, 165.7, 159.6, 181.2, 176.8 and 208.6 kJ mol^{-1}, respectively.

Conclusions

From analytical and thermoanalytical (TG) results a general formula could be established for these compounds in the solid state.

The X-ray powder patterns showed that all the compounds synthesized showed low crystallinity degree.

The infrared spectroscopic data suggest that the $C_4H_4O_6$ acts as a ligand towards the metal ions.

The TG-DTA and DSC curves provided previously underported information concerning the thermal behaviour and thermal decomposition of these compounds.

Acknowledgements The authors thank FAPESP, CAPES and CNPq Foundations (Brazil) for financial support.

References

1. Evangelista J. Tecnologia de alimentos. São Paulo: Editora Atheneu; 1999. p. 49.

2. Rizzon LA, Miele A. Concentração de ácido tartárico nos vinhos da Serra Gaúcha. Cienc Rural, Santa Maria. 2001;31:893–5.
3. Want B, Ahmad F, Kotru PN. Crystal growth and characterization of gadolinium tartrate trihydrate: $Gd(C_4H_4O_6)(C_4H_5O_6)\cdot 3H_2O$. Mater Sci Eng A. 2006;431:237.
4. Sharma RM, Kaul ML. Thermal decomposition and kinetics of dehydration of praseodymium(III) tartarate hexahydrate. J Ind Chem Soc. 1990;67:706.
5. Sharma RM, Kaul ML. TG and DSC studies on Sm(III) and Tb(III) tartrates. J Thermal Anal Calorim. 1989;35:2143–52.
6. Deb N. Thermal decomposition behaviour of lanthanum(III) tristartrato lanthanate(III) decahydrate. J Therm Anal Calorim. 2004; 78:227–37.
7. Bamzai KK, Kumar S. Studies on kinetics and mechanism of thermal decomposition of yttrium tartrate trihydrate crystals. Mater Chem Phys. 2008;107:200–7.
8. Arora SK, Patel V, Kothari A. Kinetics and mechanism of thermal decomposition of strontium tartrate crystals. Mater Chem Phys. 2004;84:323–30.
9. Ambrozini B, Dametto PR, Siqueira AB, Carvalho CT, Ionashiro M. Synthesis, characterization and thermal behavior on solid tartrates of light trivalent lanthanides. J Therm Anal Calorim. 2009;97:761–4.
10. Ionashiro M, Graner CAF, Zuanon Netto J. Titulação complexométrica de lantanídeos e ítrio. Ecl Quim. 1983;8:29–32.
11. Sócrates G. Infrared characteristic group frequencies. 2nd ed. New York: Wiley; 1994.
12. Silverstein RM, Webster FX. Spectrometric identification of organic compounds. 6th ed. New York: Wiley; 1998.
13. Deacon GB, Phillips RJ. Relationships between the carbon-oxygen stretching frequencies of carboxylate complexes and the type of carboxylate coordination. Coord Chem Rev. 1980;33:227–50.